A Systematic Evaluation of Molecular Recognition Phenomena. 1. Interaction between Phosphates and Nucleotides with Hexaazamacrocyclic Ligands Containing *m*-Xylylic Spacers

Carmen Anda, Antoni Llobet,* and Victoria Salvado

Departament de Química, Universitat de Girona, Campus de Montilivi 17071, Girona, Spain

Joseph Reibenspies, Ramunas J. Motekaitis, and Arthur E. Martell*

Department of Chemistry, Texas A&M University, College Station, Texas 77843-3255

Received July 9, 1999

The host−guest interactions between ortho- (Ph), pyro- (Pp), and tripolyphosphate (Tr) anions together with ATP (At), ADP (Ad), and AMP (Am) nucleotides and the hexaazamacrocyclic ligand 3,7,11,19,23,27-hexaazatricyclo[27.3.1.1^{13,17}]triaconta-1(32),13,15,17(34),29(33),30-hexaene (Bn) have been investigated by potentiometric equilibrium methods. Ternary complexes are formed in aqueous solution as a result of hydrogen bond formation and Coulombic attraction between the host and the guest. Formation constants for all the species obtained are reported. The selectivity of the Bn ligand with regard to the phosphate and nucleotide substrates is discussed and illustrated with species distribution diagrams. A comparison of the present results with those obtained for the similar but smaller macrocyclic ligand 3,6,9,17,20,23-hexaazatricyclo[23.3.1.1^{11,15}]triaconta-1(29),11(30),12,14,25,27-hexaene (Bd) is also discussed. It is found that the competition of the Bd and Bn ligands for the formation of ternary species with a specific substrate is strongly dependent on the p[H]. The crystal structure of the compound $[(H_6Bn)(H_2PO_4)_6]\cdot 2H_2O$ with empirical formula $C_{28}H_{68}N_6O_{26}P_6$ has been solved by means of X-ray diffraction analysis. The compound belongs to the triclinic $P\bar{1}$ space group with $Z = 1$, $a = 8.892(2)$ Å, $b = 9.369(4)$ Å, $c = 16.337(8)$ Å, $\alpha = 73.72(4)°$, $\beta = 83.01(4)°$, and $\gamma = 64.81(3)°$. The phosphate counterions are found to bridge adjacent layers of macrocyclic molecules through an extensive hydrogen-bonding network.

Introduction

Anion coordination chemistry is a rapidly emerging field stimulated by the continuous interest displayed in anions by researchers from environmental, industrial, and health-related domains.[1] Recently, anion receptors have been applied in separation membranes, in anion transport, and in the construction of ion-selective electrodes.[2]

Phosphate anions are ubiquitous in biological structure, function, and regulation; thus, their interaction with their corresponding receptors is of special interest.[3] Polyazamacrocyclic ligands, in their protonated forms, have been shown to bind certain neutral molecules and anions including phosphates in aqueous solution and in the solid state.[4] Furthermore such macrocyclic ligands have also been reported to catalyze biologically significant reactions of their bonded guests,[1c−5] such as ATP hydrolysis and formation.

(1) For selected recent reviews see: (a) Martell, A. E. In *Crown Compounds: Towards Future Applications*; Cooper, S. R., Ed.; VCH Publishers: New York, 1992; Chapter 7, pp 99−134. (b) In *Supramolecular Chemistry of Anions*; Bianchi, A., Bowman-James, K., García-España, E., Eds.; Wiley-VCH: New York, 1997. (c) Mertes, M. P.; Mertes, K. B. *Acc. Chem. Res.* **1990**, *23*, 413−418. (d) Beer, P. D.; Wheeler, J. W.; Moore, C. In *Supramolecular Chemistry*; Balzani, V., De Cola, L., Eds.; Kluwer Academic Publishers: Dordrecht, The Netherlands, 1992; pp 105−118. (e) Katz, H. E. In *Inclusion Compounds*; Atwood, J. L., Davies, J. E. D., MacNichol, D. D., Eds.; Oxford University Press: Oxford, U.K., 1991; pp 391−405. (f) Dietrich, B. *Pure Appl. Chem.* **1993**, *65*, 1457−1464. (g) Izatt, R. M.; Pawlak, K.; Bradshaw, J. S.; Bruening, R. L. *Chem. Rev.* **1991**, *91*, 1721−2085.

(2) Antonisse, M. M. G.; Reinhoudt, D. N. *Chem. Commun.* **1998**, 443−448.

(3) Kanyo, Z. F.; Christianson, D. W. *J. Biol. Chem.* **1991**, *266*, 4264−4268.

(4) (a) Aguilar, J. A.; García-España, E.; Guerrero, J. A.; Luis, S. V.; Llinares, J. M.; Miravet, J. F.; Ramírez, J. A.; Soriano, C. *J. Chem. Soc., Chem. Commun.* **1995**, 2237. (b) Lu, Q.; Motekaitis, R. J.; Reibenspies, J. H.; Martell, A. E. *Inorg. Chem.* **1995**, *34*, 4958. (c) Llobet, A.; Riebenspies, J.; Martell, A. E. *Inorg. Chem.* **1994**, *33*, 5946. (d) Motekaitis, R. J.; Martell, A. E. *Inorg. Chem.* **1992**, *31*, 5534. (e) Dietrich, B.; Hosseini, M. W.; Lehn, J.-M.; Sessions, B. R. *J. Am. Chem. Soc.* **1981**, *103*, 1282. (f) Jahansouz, H.; Jiang, Z.; Himes, R. H.; Mertes, K. B.; Mertes, M. P. *J. Am. Chem. Soc.* **1989**, *111*, 1409. (g) Bazzicalupi, C.; Bencini, A.; Bianchi, A.; Cecchi, M.; Escuder, B.; Fusi, V.; García-España, E.; Giorgi, C.; Luis, S. V.; Macagni, G.; Marcelino, V.; Paoletti. P.; Valtancoli, B. *J. Am. Chem. Soc.* **1999**, *121*, 6807.

(5) (a) Hosseini, M. W.; Lehn, J.-M.; Mertes, M. P. *Helv. Chim. Acta* **1983**, *66*, 2454. (b) Hosseini, M. W.; Lehn, J.-M.; Maggiora, L.; Mertes, K. B.; Mertes, M. P. *J. Am. Chem. Soc.* **1987**, *109*, 537. (c) Hosseini, M. W.; Lehn, J.-M. *Helv. Chim. Acta* **1987**, *70*, 1312. (d) Hosseini, M. W.; Lehn, J.-M. *J. Am. Chem. Soc.* **1987**, *109*, 7047. (e) Blackburn, G. M.; Thatcher, G. R. J.; Hosseini, M. W.; Lehn, J.-M. *Tetrahedron Lett.* **1987**, *28*, 2779. (f) Hosseini, M. W.; Lehn, J.-M.; Jones, K. C.; Plute, K. E.; Mertes, K. B.; Mertes, M. P. *J. Am. Chem. Soc.* **1989**, *111*, 6330. (g) Hosseini, M. W.; Blacker, A. J.; Lehn, J.-M. *J. Am. Chem. Soc.* **1990**, *112*, 3896. (h) Bencini, A.; Bianchi, A.; García-España, E.; Scott, E. C.; Morales, L.; Wang, B.; Deffo, T.; Takusagawa, F.; Mertes, M. P.; Mertes, K. B.; Paoletti, P. *Bioorg. Chem.* **1992**, *20*, 8. (i) Andrés, A.; Aragó, J.; Bencini, A.; Bianchi, A.; Domenech, A.; Fusi, V.; García-España, E.; Paoletti, P.; Ramírez, J. A. *Inorg. Chem.* **1993**, *32*, 3418. (j) Bencini, A.; Bianchi, A.; Giorgi, C.; Paoletti, P.; Valtancoli, B., Fusi, V.; García-España, E.; Llinares, J. M.; Ramírez, J. A. *Inorg. Chem.* **1996**, *35*, 1114. (k) Lu, Q.; Martell, A. E.; Motekaitis, R. J. *Inorg. Chim. Acta* **1996**, *251*, 365.

10.1021/ic990818p CCC: $19.00 © 2000 American Chemical Society
Published on Web 06/14/2000

Table 1. Crystal Data for the Complex $(H_6Bn)(H_2PO_4)_6$

chem formula	$C_{28}H_{56}N_6O_{26}P_6$
fw	1078.6
cryst system, space group	triclinic, $P\bar{1}$
a, Å	8.982(3)
b, Å	9.369(4)
c, Å	16.337(8)
α, deg	72.72(4)
β, deg	83.01(4)
γ, deg	64.81(3)
V, Å^3	1182.2(9)
formula units/cell	1
temp, K	293(2)
λ(Mo Kα), Å	0.710 73
ρ_{calc}, g/cm^3	1.515
μ, mm^{-1}	0.320
R^a	0.0477
$R_w{}^b$	0.1161

^{a} $R = \sum||F_o| - |F_c||/\sum|F_o|$. ^{b} $R_w = [\sum[w(F_o^2 - F_c^2)^2/\sum[w(F_o^2)^2]]^{1/2}$.

Table 2. Selected Bond Lengths (Å) and Bond Angles (deg) for the Complex $(H_6Bn)(H_2PO_4)_6$

P(1)−O(1)	1.495(2)	P(1)−O(2)	1.502(2)
P(1)−O(3)	1.562(3)	P(1)−O(4)	1.567(3)
P(2)−O(5)	1.493(2)	P(2)−O(7)	1.503(3)
P(2)−O(8)	1.556(3)	P(2)−O(6)	1.583(3)
P(3)−O(10)	1.502(2)	P(3)−O(12)	1.505(2)
P(3)−O(9)	1.563(2)	P(3)−O(11)	1.569(3)
N(1)−C(2)	1.484(4)	N(1)−C(1)	1.506(4)
N(2)−C(5)	1.491(4)	N(2)−C(4)	1.496(4)
N(3)−C(7)	1.493(4)	N(3)−C(8)	1.515(4)
O(1)−P(1)−O(2)	116.88(14)	O(1)−P(1)−O(3)	107.8(2)
O(2)−P(1)−O(3)	109.63(14)	O(1)−P(1)−O(4)	104.61(15)
O(2)−P(1)−O(4)	110.75(15)	O(3)−P(1)−O(4)	106.6(2)
O(5)−P(2)−O(7)	116.9(2	O(5)−P(2)−O(8)	110.35(14)
O(7)−P(2)−O(8)	109.3(2)	O(5)−P(2)−O(6)	108.68(15)
O(7)−P(2)−O(6)	106.37(14)	O(8)−P(2)−O(6)	104.4(2)
O(10)−P(3)−O(12)	114.18(14)	O(10)−P(3)−O(9)	108.92(14)
O(12)−P(3)−O(9)	111.15(15)	O(10)−P(3)−O(11)	109.34(15)
O(12)−P(3)−O(11)	109.32(14)	O(9)−P(3)−O(11)	103.4(2)

Recently the complexes formed between various protonated forms of the hexaazamacrocyclic ligand 3,6,9,17,20,23-hexaazatricyclo[23.3.1.1^{11,15}]triaconta-1(29),11(30),12,14,25,27-hexaene (Bd) and the series of anions derived from phosphoric, diphosphoric, and triphosphoric acid together with ATP, ADP, and AMP were reported.[6] Stable binary complexes were formed as a result of Coulombic interactions and hydrogen bonding.

To get a deeper understanding of the host−guest interaction between this type of receptor and phosphate type of substrates we decided to evaluate the binding constants of binary complexes formed by Bd and 3,7,11,19,23,27-hexaazatricyclo-[27.3.1.1^{13,17}]triaconta-1(32),13,15,17(34),29(33),30-hexaene (Bn). Bn is also a hexaazamacrocyclic ligand with a structure similar to Bd but with a larger cavity.

Here we report a systematic evaluation of recognition phenomena, based on potentiometric equilibrium methods, with the protonated forms of Bn and phosphate type of substrates together with a comparison of the results obtained previously with Bd.

Experimental Section

Materials. The ligand Bn was prepared as a colorless hexabromide salt according to a published procedure.[4c] GR grade KCl was obtained from EM Chemical Co., and CO_2-free Dilut-it ampules of KOH were purchased from J. T. Baker Inc. Reagent grade potassium dihydrogen phosphate and tetrasodium pyrophosphate were purchased from Fischer Scientific Co. and further purified by recrystallization from distilled water. Sodium tripolyphosphate (technical grade, 85%) was purchased from Aldrich Chemical Co. and was purified by repeated crystallization from aqueous solution by the addition of methanol.[7] Adenosine-5′-monophosphate, adenosine-5′-diphosphate sodium salt hydrate, and

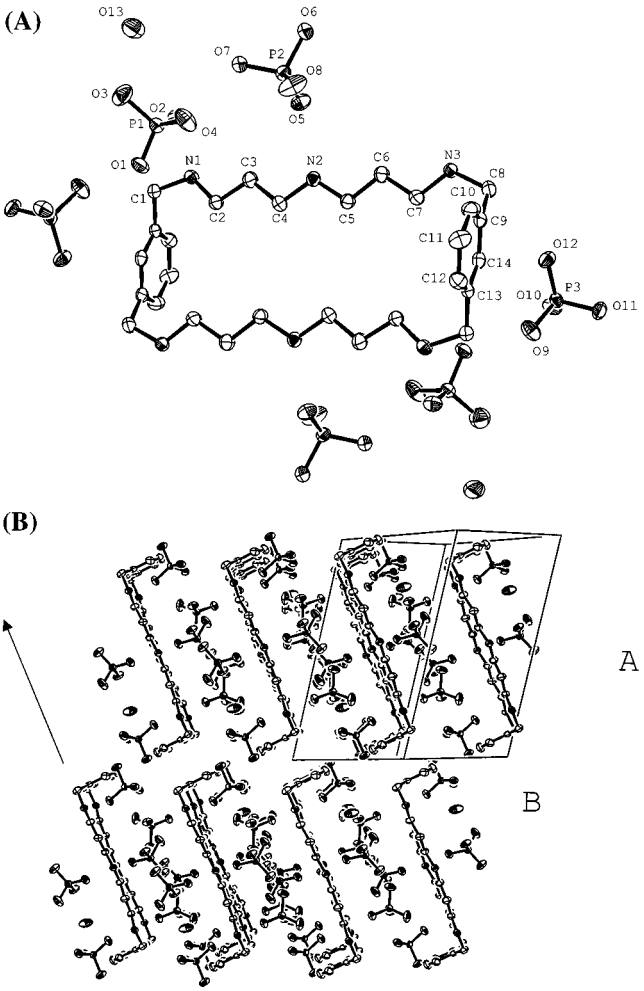

Figure 1. (A) ORTEP view (thermal ellipsoids at 50% probability) of the molecular structure of $(H_6Bn)(H_2PO_4)_6$ including the atom numbering scheme. (B) View of the crystal packing of $(H_6Bn)(H_2PO_4)_6$ along two unit cells in the x, y, and z directions.

Chart 1

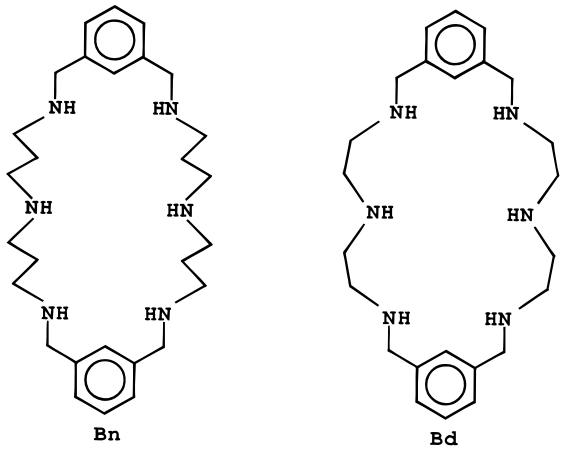

(6) (a) Nation, D. A.; Riebenspies, J. H.; Martell, A. E. *Inorg. Chem.* **1996**, *35*, 4597. (b) Nation, D. A.; Lu, Q.; Martell, A. E. *Inorg. Chim. Acta* **1997**, *263*, 209.

(7) Watters, J. I.; Loughran, E. D.; Lambert, S. M. *J. Am. Chem. Soc.* **1956**, *78*, 4855.

Table 3. Logarithm Protonation Constants of the Ligands Bn and Bd and the Related Triamines Dipropylenetriamine (dpt), Ethylenepropylenetriamine (ept), and Diethylenetriamine (det)

equilib quotient	Bn[a]	Bd	dpt	ept	det
$K^H_1 = [HL]/[L][H]$	10.33	9.51	10.65	10.21	9.84
$K^H_2 = [H_2L]/[HL][H]$	9.73	8.77	9.57	9.17	9.02
$K^H_3 = [H_3L]/[H_2L][H]$	8.56	7.97	7.69	6.10	4.26
$K^H_4 = [H_4L]/[H_3L][H]$	7.77	7.09			
$K^H_5 = [H_5L]/[H_4L][H]$	7.22	3.79			
$K^H_6 = [H_6L]/[H_5L][H]$	6.64	3.27			
$\sum \log K^H_i$	50.24	40.40	27.94	25.48	23.09
ref	this work	6a	9	9	9

[a] Our data agree very well with that reported previously in ref 4c.

adenosine-5′-triphosphate disodium salt hydrate were purchased from Aldrich Chemical Co. ATP was recrystallized from methanol and water; ADP and AMP were used as received. The KOH solution was standardized by titration against standard potassium acid phthalate with phenolphthalein as indicator and was checked periodically for carbonate content (<2%).[8]

Potentiometric Titrations. Potentiometric measurements were conducted in a jacketed cell thermostated at 25.0 °C and kept under an inert atmosphere of purified argon. A Corning model 350 pH meter fitted with glass and calomel reference electrodes was used. KCl was employed as supporting electrolyte to maintain the ionic strength at 0.10 M. The apparatus was calibrated in terms of $-\log [H^+]$, designated as p[H], by titration of a small quantity of diluted HCl at 0.10 M ionic strength and 25 °C followed by adjustment of the meter so as to minimize the calculated p[H] vs observed values. $\log K_w$ for the system, defined in terms of $\log([H^+][OH^-])$, was found to be -13.78 at the ionic strength employed[9] and was maintained fixed during refinements.

Potentiometric measurements of solutions containing equimolecular amounts of Bn and the appropriate phosphate or nucleotide anion were made at concentrations approximately 1 mM and ionic strength μ = 0.10 M (KCl). Each titration utilized at least 10 points per neutralization of a hydrogen ion equivalent, with titrations being repeated until satisfactory agreement was obtained. A minimum of three sets of data was used in each case to calculate the overall stability constants and their standard deviations. The range of accurate p[H] measurements were considered to be 2−12. Equilibrium constants and species distribution diagrams were calculated using the programs BEST[8a] and SPEXY, respectively.[8b]

Crystal Structure Determination. Preparation of $(H_6Bn)(H_2PO_4)_6$. Small colorless crystals of the hexaphosphate salt were obtained upon slow evaporation at room temperature of an aqueous solution containing $(H_6Bn)Br_6$ with an excess of potassium dihydrogen phosphate. A colorless plate (0.1 × 0.3 × 0.3) was mounted on a glass fiber at room temperature. Preliminary examination and data collection were performed on a Siemens R3M (oriented graphite monochromator; Mo Kα radiation) at 293(2) K. Cell parameters were calculated from the least-squares fitting for 25 high-angle reflections ($2\theta > 15°$). ω scans for several intense reflections indicated acceptable crystal quality. Data were collected for 4.96 to 50.00° in 2θ at 293(2) K. Scan width for data collection was 2.0 deg in ω with a variable scan rate between 3.0 and 14.0°/min. The three standards, collected every 97 reflections, showed no significant trends. Background measurement by stationary crystal and stationary counter technique at the beginning and the end of each scan for $^1/_2$ the total scan time.

Lorentz and polarization corrections were applied to 4330 reflections. A semiempirical absorption correction was applied. A total of 4169 unique reflections (R_{int} = 0.0398) were used in further calculations. The structure was solved by Direct Methods (Sheldrick, 1997).[10a] Full-matrix least-squares anisotropic refinement for all non-Hydrogen atoms yielded $R(F)[I > 2\sigma(I)] = 0.048$ and $wR(F^2)$[all data] = 0.1354 at convergence (Sheldrick, 1997).[10b] Hydrogen atoms were placed in idealized positions with isotropic thermal parameters fixed 1.2 or 1.5 times the value of the attached atom. Neutral atom scattering factors and anomalous scattering factors were taken from ref 10c.

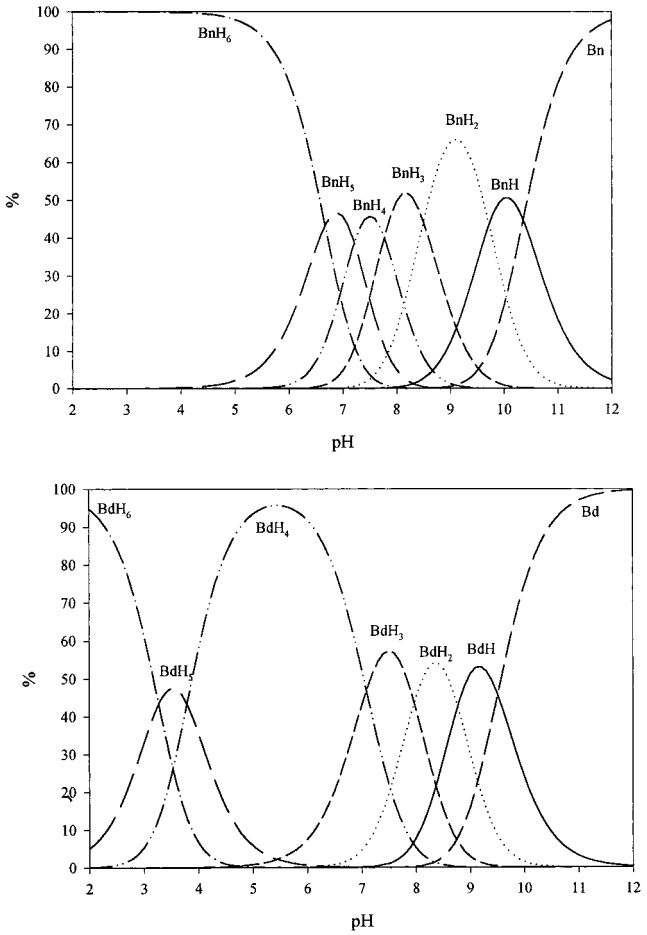

Figure 2. Species distribution diagram for the Bn and Bd ligands as a function of p[H].

Results and Discussion

Synthesis and Structure of $(H_6Bn)(H_2PO_4)_6$. The $(H_6Bn)(H_2PO_4)_6$ complex was obtained when an excess of potassium dihydrogen phosphate was added to an aqueous solution containing H_6BnBr_6.[4c]

$$H_6BnBr_6 + 6H_2PO_4^- \rightarrow (H_6Bn)(H_2PO_4)_6 + 6Br^-$$

The structure of $(H_6Bn)(H_2PO_4)_6$ has been determined by means of monocrystal X-ray diffraction analysis. A summary of the data collection and refinement parameters is given in Table 1. Selected bond distances and angles is given in Table 2. Figure 1A displays the thermal ellipsoid plot, with 50% probability, of $(H_6Bn)(H_2PO_4)_6$ together with the atomic labeling scheme while Figure 1B shows a diagram of the molecular crystal

(8) (a) Martell, A. E.; Motekaitis, R. J. *Determination and Use of Stability Constants*, 2nd ed.; John Wiley and Sons: New York, 1992. (b) SPEXY is a program created by R.J.M. which generates an X−Y file that contains the concentration of all the existent species in solution as a function of p[H] using BEST output files.

(9) Smith, R. M.; Martell, A. E. *NIST Critically Selected Stability Constants: Version 2.0*; National Institute of Standards and Technology: Gaithersburg, MD, 1995.

(10) (a) Sheldrick, G. *SHELXS-97 Program for Crystal Structure Solution*; Institut fur Anorganische Chemie der Universitat: Tammanstrasse 4, D-3400 Gottingen, Germany, 1997. (b) Sheldrick, G. *SHELXL-97 Program for Crystal Structure Refinement*; Institut fur Anorganische Chemie der Universitat: Tammanstrasse 4, D-3400 Gottingen, Germany, 1997. (c) *International Tables for Crystallography*; Wilson, A. J. C., Ed.; Kluwer Academic Publishers: Dordecht, The Netherlands, 1992; Vol. C, Tables 4.2.6.8 (pp 219−222) and 6.1.1.4 (pp 500−502).

Chart 2. Formulas for Phosphate and Nucleotide Substrates and Their Corresponding Abbreviations Used in the Present Work

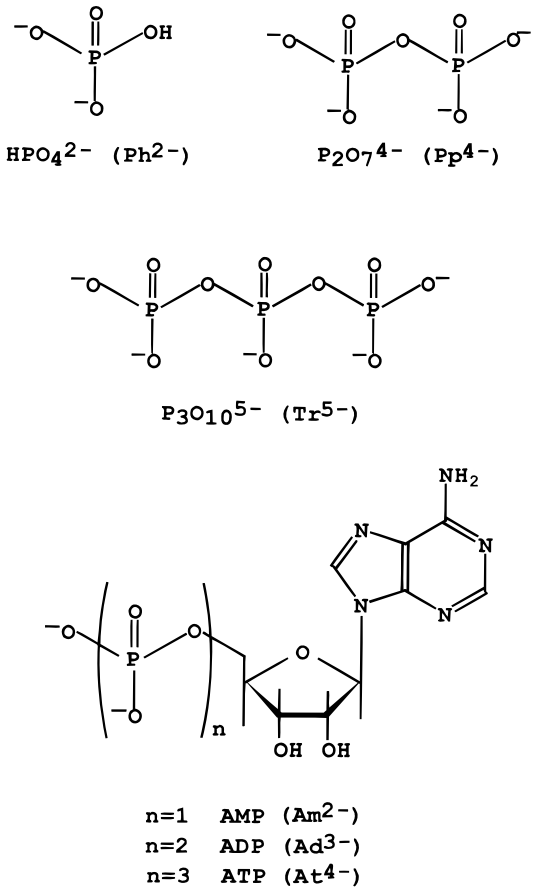

packing along two cell units in the *x*, *y*, and *z* directions. There is only one molecule per unit cell, and the crystal structure belongs to the space group $P\bar{1}$, with the crystallographic inversion center located inside the macrocyclic cavity. This cavity can be described as a rectangle where its corners are occupied alternately by C1 and C8 atoms thus leading to a cavity with a length of 12.89 Å and a width of 4.98 Å. The three nitrogen atoms of each macrocyclic arm are linearly accommodated in a plane that contains the rest of the aliphatic carbons. The planarity is achieved because of a zigzag type of arrangement of successive N and C atoms. The latter indicates that all hydrogen atoms either from aliphatic C or N point above and below the plane defined by the macrocyclic cavity. The phenyl rings are nearly perpendicular to that plane (approximately 83−84°) and at the same time are parallel with respect to one another pointing in opposite directions. The three crystallographically distinct phosphate moieties anions have relatively similar geometries. For instance, the phosphate anion containing the P1 phosphorus atom has two short and two long P−O bond distances (P1−O1 = 1.495 Å, P1−O2 = 1.502 Å, P1−O3 = 1.562 Å, P1−O4 = 1.567 Å). This suggests that O1 and O2 share the negative charge and form hydrogen bonds with the hexaprotonated Bn ligand while O3 and O4 are bonded to their corresponding hydrogen atoms. The phosphate anions are bonded to the macrocyclic cation through extensive hydrogen bonding that takes place between the nitrogen atoms of the Bn^{6+} cation and one of the oxygen atoms of each phosphate moiety. The distances between hydrogen-bonded atoms range from 2.69 to 2.85 Å. Thus they are considered to be medium to strong hydrogen bonds (O2−N1 = 2.715 Å, O2−N3′ = 2.798 Å; O5−N2 = 2.849 Å, O5−N2′ = 2.744 Å; O10−N1′ = 2.689 Å, O10−N3″ = 2.701 Å; the prime indicates nitrogen atoms from neighboring macrocyclic molecules). Thus each hydrogen-bonded oxygen atom interacts with two different nitrogen atoms from two distinct neighboring macrocyclic molecules and consequently each nitrogen atom is hydrogen bonded to two different phosphate anions as shown in the following drawing:

Table 4. Logarithm Protonation Constants of the Phosphate and Nucleotide Substrates

equilib quotient	Tr	Pp	Ph	At	Ad	Am
$K^H_1 = [HS]/[S][H]$	7.79	8.42	11.63	6.50	6.35	6.21
$K^H_2 = [H_2S]/[HS][H]$	5.51	6.00	6.75	3.90	3.88	3.81
$K^H_3 = [H_3S]/[H_2S][H]$	1.86	1.69	1.89			

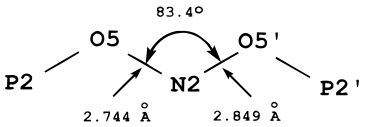

This hydrogen-bonding network is extended over the whole crystal structure as can be observed in Figure 1B. In the crystal, the macrocyclic ligands form layered structures perpendicular to plane of the paper as drawn in Figure 1B and following the direction of a hypothetical *axis* delineated by the macrocyclic arms (see the arrow in Figure 1B); this arrangement is repeated over the whole crystal structure. Within a layer and perpendicular to the defined axis, the macrocycles pile up one next to the other along the plane in the same direction with a distance of approximately 4.67 Å. Parallel to the defined axis the packing of macrocyclic ligands is still parallel with respect to one another, with the distance between the planes defined by the closest phenyl rings of each Bn being 3.53 Å. In contrast, the arrangement of macrocycle type A with regard to type B is shifted by 2.58 Å below and 3.72 Å perpendicular to the defined hypothetical axis thus avoiding $\pi-\pi$ interactions between phenyl rings. The negative phosphates also form a layer. In the crystal structure there are parallel alternate layers of macrocycles and phosphate anions that are bonded to one another through the hydrogen bonding described above.

Potonation Constants of the Ligands and Substrates. The systems described in the present work contain the hexaazamacrocyclic ligands Bn and Bd (Chart 1), which have six secondary amines. These two macrocycles have *m*-xylylic spacers and differ from one another in the length of their connecting arms. Bn is a 28-member ring macrocycle while Bd is the homologous 24-member ring, thus with a smaller cavity.

Table 3 contains the logarithms of the stepwise protonation constants for the ligands Bn and Bd as well as the protonation constants for related triamines, namely dipropylenetriamine (dpt), ethylenepropylenetriamine (ept), and diethylenetriamine (det). The six protonation constants for Bn and Bd have been calculated from the mathematical treatment of their potentiometric curves.[4c,6a] Bn has six moderate to strong basic sites as can be inferred from the protonation constants whereas Bd has four strong to moderately basic amines and two weak ones.

As it can be observed in Table 3, the number of methylenic units bonded within each secondary amine mainly determines the basicity of the ligand. As the number of methylenic units increases, the basicity of the ligands also increases due to the inductive effects of the CH_2 units and also because the protonated ammonium groups lie farther apart from one another. This is further corroborated by the protonation constants of the free amines corresponding to the arms, where a similar trend is observed as shown in Table 3.

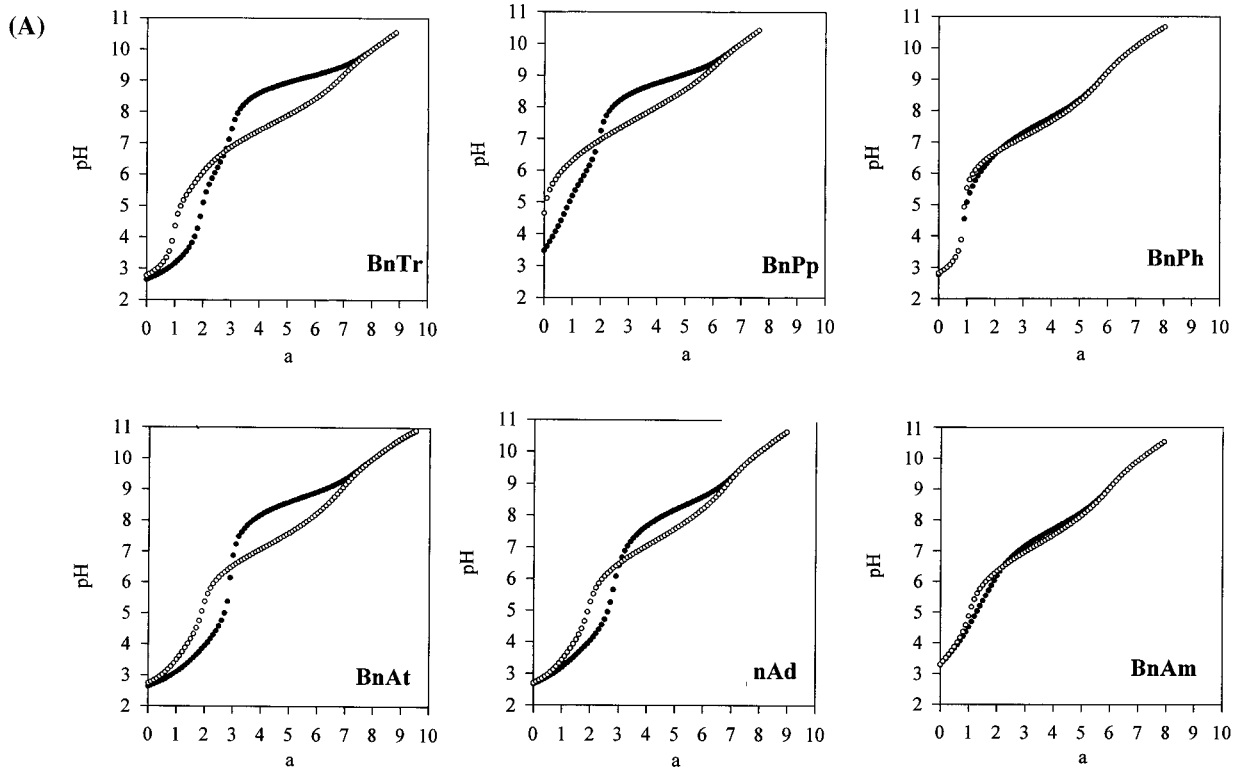
(A)
BnTr
BnPp
BnPh
BnAt
nAd
BnAm
pH
a

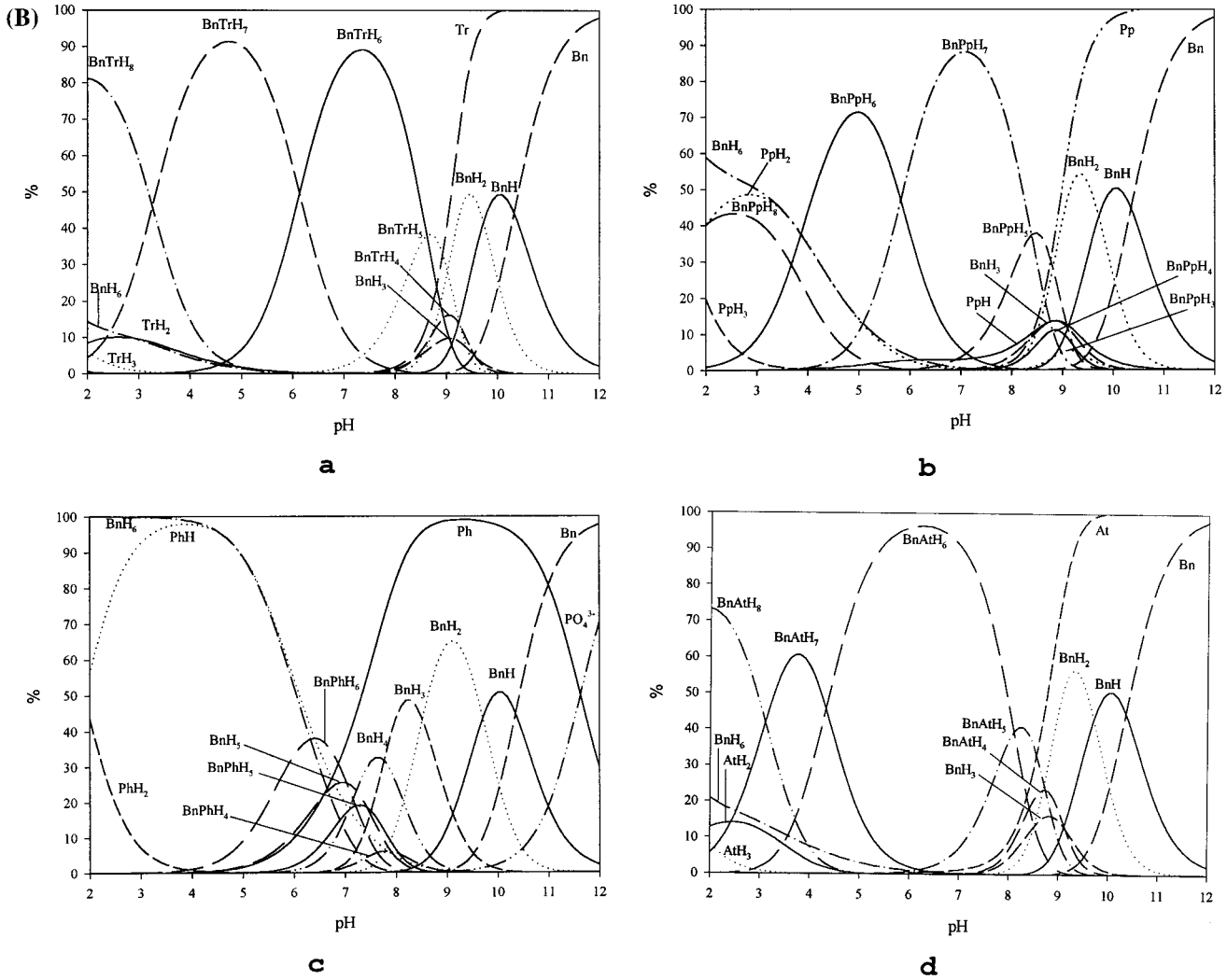
(B)
BnTrH8
BnTrH7
BnTrH6
Tr
Bn
BnH2
BnH
BnTrH5
BnTrH4
BnH3
BnH6
TrH2
TrH3
%
pH
a
BnH6
PpH2
BnPpH8
BnPpH7
BnPpH6
Pp
Bn
BnH2
BnH
BnPpH2
BnH3
BnPpH4
PpH
BnPpH3
PpH3
b
BnH6
PhH
Ph
Bn
PO4 3-
BnH2
BnH
BnPhH6
BnH3
BnH5
BnH4
BnPhH5
PhH2
BnPhH4
c
BnAtH8
BnAtH6
At
Bn
BnAtH7
BnH2
BnH
BnAtH5
BnH6
BnAtH4
AtH2
BnH3
AtH3
d

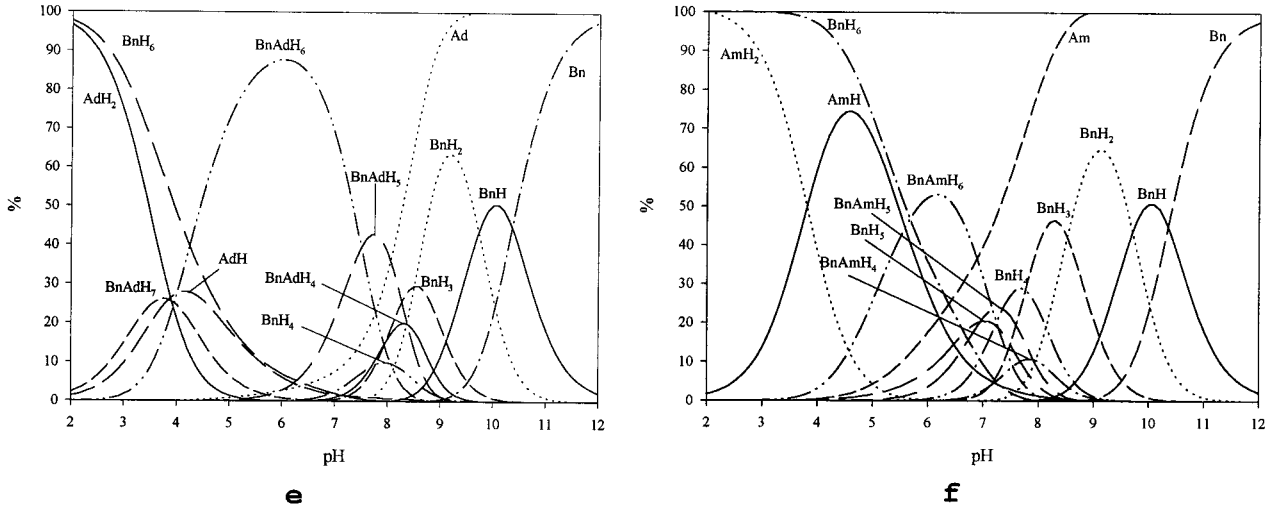

Figure 3. (A) (●) Experimental curves obtained for the potentiometric titrations of equilibrated phosphate or nucleotide substrates (1.0×10^{-3} M) with the ligand Bn (1.0×10^{-3} M) at 25 °C and $\mu = 0.1$ M (KCl) and (○) calculated potentiometric curve for the same system assuming there is no interaction between the substrate and the ligand. (B) Species distribution diagram as a function of p[H] for the six Bn−substrate systems.

Table 5. Logarithm Recognition Constants, log K^{R}_{i}, for the Bn−S[a] and Bd−S[b] Systems

stoichiometry L:S:H	equilib quotient	Tr	Pp	Ph	At	Ad	Am
			L = Bn				
1:1:1	[HBnS]/[HBn][S]						
1:1:2	$[H_2BnS]/[H_2Bn][S]$						
1:1:3	$[H_3BnS]/[H_3Bn][S]$		2.57		2.59		
1:1:4	$[H_4BnS]/[H_4Bn][S]$	4.56	4.12	2.13	4.07	3.39	2.42
1:1:5	$[H_5BnS]/[H_5Bn][S]$	6.61	6.13	2.96	5.76	4.54	3.11
1:1:6	$[H_6BnS]/[H_6Bn][S]$	8.60	7.85	3.50	7.13	5.37	3.62
1:1:7	$[H_7BnS]/[H_6Bn][HS]$	6.76	5.25		4.97	2.98	
1:1:8	$[H_8BnS]/[H_6Bn][H_2S]$	4.52	2.93		4.20		
	$1000\sigma_{fit}$	4.2	1.8	3.7	3.7	8.1	6.5
			L = Bd				
1:1:1	[HBdS]/[HBd][S]	3.51					2.10
1:1:2	$[H_2BdS]/[H_2Bd][S]$						2.20
1:1:3	$[H_3BdS]/[H_3Bd][S]$	4.71			3.35	3.07	2.70
1:1:4	$[H_4BdS]/[H_4Bd][S]$	6.47	5.73	2.87	5.27	4.37	3.33
1:1:5	$[H_5BdS]/[H_5Bd][S]$	10.85	9.94	5.47	8.69	7.42	5.60
1:1:6	$[H_6BdS]/[H_6Bd][S]$	14.19	13.07	7.36	11.16	9.47	7.12
1:1:7	$[H_7BdS]/[H_6Bd][HS]$	11.06	6.14		7.88	6.24	3.80
1:1:8	$[H_8BdS]/[H_6Bd][H_2S]$	7.57			5.42		

[a] Data from this work. [b] Data from ref 6.

Figure 2 shows the species distribution diagrams for Bn and Bd based on the constants reported in Table 3. For Bn, the H_6L^{6+} species predominates from the p[H] range 2−6 and the H_5L^{5+} species does not significantly start to form until p[H] = 5. At higher p[H] (7−10) the remaining lower protonation species are expressed. For Bd the zone of predominance of the H_6L^{6+} is reduced by 3 log units within the p[H] range 2−3. In this case the H_5L^{5+} species is significantly formed even at p[H] = 2. As a result of the shifting to lower p[H], the H_4L^{4+} species predominates over the p[H] range 4−7 and from p[H] 5 to 6 is practically the only present species. In sharp contrast for the Bn ligand the H_4L^{4+} species predominate only within the narrow p[H] range 7.2−7.7. As the p[H] is increased from 7 to 10 the rest of the lower protonated species progressively emerge.

The stepwise protonation constants for Bn do not differ by more than 1 log unit from one another as the ligand is progressively protonated. For the Bd ligand the former is true except for the fifth protonation constant which differs in more than 3 log units. This is as a result of the lesser basicity of the Bd ligand as the number of methylenic units is decreased by four with regard to Bn. The overall basicity of the ligands also reflects these effects; for Bn log β_6 (Σlog K^{H}_{i}) is 50.24 while for Bd it is 40.40. Therefore each methylenic unit contributes roughly by 2.5 log units to the overall basicity of the ligand.

Up to the fourth protonation constant, the positive charges can be relatively apart from one another and therefore the constants in the Bn and Bd ligands differ by less than 1 log unit. In sharp contrast, the fifth and sixth protonation constants are largely affected by the nature of their arms. This is a result of a combination of an electronic effect produced by the inductive capacity of the methylenic units and a spatial effect produced by the enlargement of the macrocyclic cavity that allows a higher separation of the positive charges of the protonated amino nitrogens.

The substrates used in the present work include three inorganic polyphosphates and their corresponding nucleotides (see Chart 2).

Table 4 presents the protonation constants for all six substrates. As can be observed in all of them only the unprotonated and monoprotonated species are moderately to strongly basic. The diprotonated species in all cases have log K values lower than 2 indicating that they are very weak bases. The fourth protonation constants for diphosphate and triphosphate are below the range of accurate measurement by regular

potentiometry. Because the protonation constants for these substrates are dependent on the medium chosen for the maintenance of the ionic strength,[1] all the constants were redetermined for this work under exact conditions employed for subsequent titrations. The log *K* values obtained this way agree very well with previously reported data in the literature.[9]

Formation of Ternary Species H:Bn:S. Figure 3A shows the experimental curves obtained for the potentiometric titrations of the phosphates and nucleotides. Together with the experimental curves, in Figure 3A the calculated curves obtained by assuming no interaction is taking place are also plotted. The divergence between the two curves irrefutably manifests the formation of complexes between the Bn ligand and the substrates. The degree of divergence in the curves is directly related to the binding strength of the generated complexes as shown mathematically through the formation constants displayed in Table 5.

Several qualitative general trends can be deduced from the titration curves exhibited in Figure 3A. At high p[H] no interaction exists between the ligand and the substrates, and therefore, the two curves merge into one. At lower p[H], the degree of divergence decreases in the order Tr > Pp > Ph for the inorganic phosphates and in a similar manner, At > Ad > Am, for the nucleotides.

With the individual protonation constants for Bn and for each substrate precisely known then the potentiometric data of a solution containing an equimolecular amount of ligand and substrate can be resolved giving the log *K* values of the species generated (see Table 5).

For the Bn−Tr system ($\sigma_{fit} = 0.0042$) the presence of five equilibrium species is detected which are expressed as follows:

$$H_4Bn^{4+} + Tr^{5-} \rightleftarrows H_4BnTr^{-} \qquad \log K^{R}_{4} = 4.56$$

$$H_5Bn^{5+} + Tr^{5-} \rightleftarrows H_5BnTr \qquad \log K^{R}_{5} = 6.61$$

$$H_6Bn^{6+} + Tr^{5-} \rightleftarrows H_6BnTr^{+} \qquad \log K^{R}_{6} = 8.59$$

$$H_6Bn^{6+} + HTr^{4-} \rightleftarrows H_7BnTr^{+} \qquad \log K^{R}_{7} = 6.76$$

$$H_6Bn^{6+} + H_2Tr^{3-} \rightleftarrows H_8BnTr^{3+} \qquad \log K^{R}_{8} = 4.52$$

Here K^{R}_{i} are the recognition constant of protonation degree *i* and are listed in order of appearance from low to high p[H].

Figure 3B shows the species distribution diagram as a function of p[H] obtained for the 1:1 Bn−substrate (for both inorganic phosphates and nucleotides) systems. For the Bn−Tr system, it is interesting to note that over the p[H] range 2−9 the predominant species are always H_iBnTr complexes rather than the individual species derived from the protonation of Bn ligand and the Tr^{5-} anion. It is also worth noting that for this system even at p[H] = 2 the complex species, H_8BnTr^{3+}, has an abundance of over 80% while the free ligand, H_6Bn^{6+}, is only about 15%.

The recognition constant values obtained for this system lay within the range of previously reported host−guest interactions with hexaazamacrocyclic amines and phosphates containing aromatic[4b−c,6,12] and aliphatic[4d,5c,13] spacers. For example, the recognition of pyrophosphate by protonated forms of 4,7,10,16,19,22-hexaaza-1,13-dioxacyclotetracosane (O-BISDIEN), a ligand composed of two diethylenetriamine moieties linked by $CH_2CH_2OCH_2CH_2$ spacers, produces log K^{R}_{i} values in the range 2.07−12.56.[12]

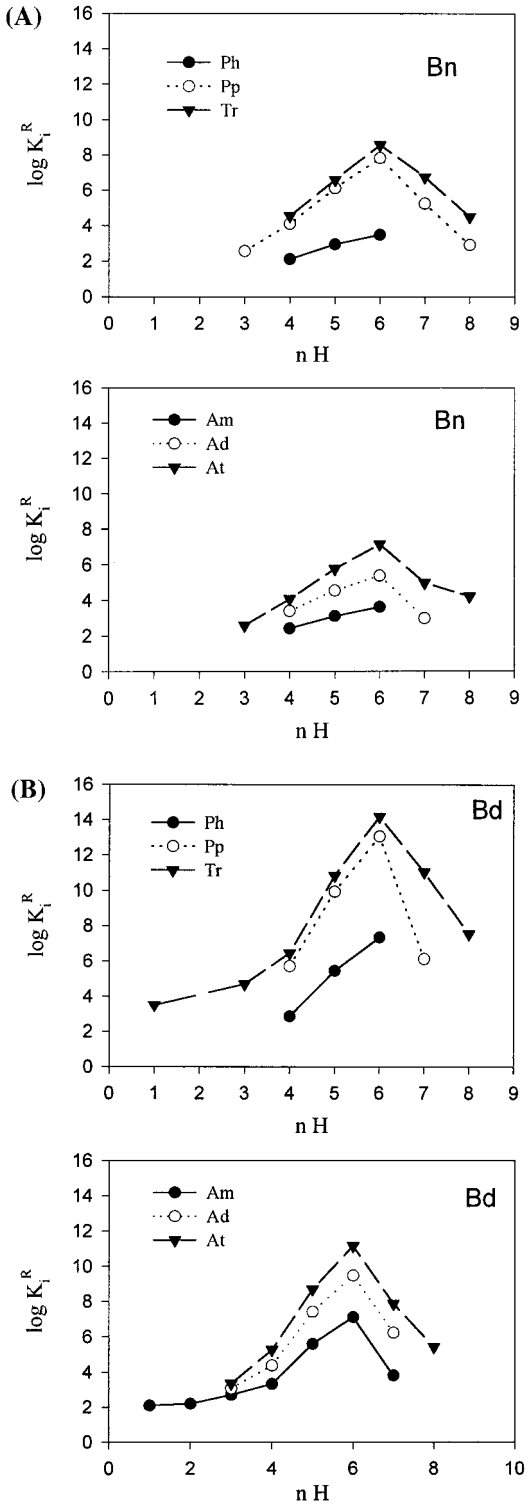

Figure 4. (A) Plot of the log K^{R}_{i} versus *n*H (the different ternary species with various degree of protonation) obtained for the Bn−S systems. (B) Similar plot but for the Bd−S systems.

(11) (a) Nation, D. A.; Martell, A. E.; Caroll, R. I.; Clearfield, A. *Inorg. Chem.* **1996**, *35*, 7246. (b) Lu, Q.; Riebenspies, J. H.; Caroll, R. I.; Martell, A. E.; Clearfield, A. *Inorg. Chim. Acta* **1998**, *270*, 207. (c) Lu, Q.; Riebenspies, J. H.; Martell, A. E.; Motekaitis, R. J. *Inorg. Chem.* **1996**, *35*, 2630.

(12) Bazzicalupi, C.; Bencini, A.; Bianchi, A.; Fusi, V.; Giorgi, C.; Granchi, A.; Paoletti, P.; Valtancoli, B. *J. Chem. Soc., Perkin Trans. 2* **1997**, 775.

(13) (a) Jurek, P. E.; Martell, A. E.; Motekaitis, R. J.; Hancock. R. D. *Inorg. Chem.* **1995**, *34*, 1823. (b) Motekaitis, R. J.; Martell, A. E. *Inorg. Chem.* **1994**, *33*, 1032. (c) English, J. B.; Martell, A. E.; Motekaitis, R. J.; Murase, I. *Inorg. Chim. Acta*, submitted for publication.

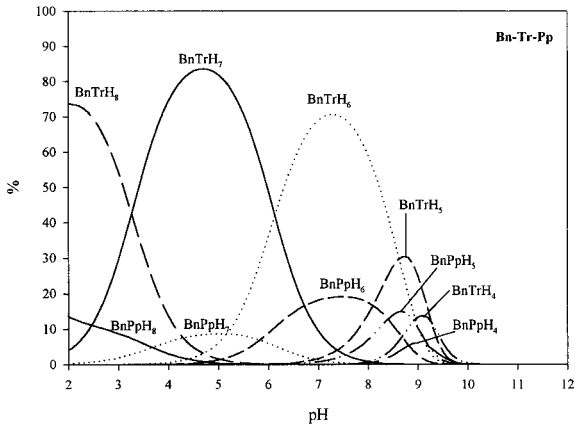
Bn-Tr-Pp
BnTrH8
BnTrH7
BnTrH6
BnTrH5
BnPpH6
BnPpH5
BnTrH4
BnPpH8
BnPpH7
BnPpH4
%
pH

a

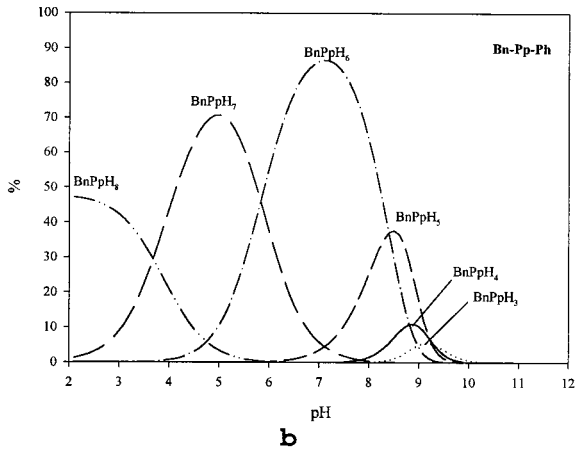
Bn-Pp-Ph
BnPpH6
BnPpH7
BnPpH8
BnPpH5
BnPpH4
BnPpH3
%
pH

b

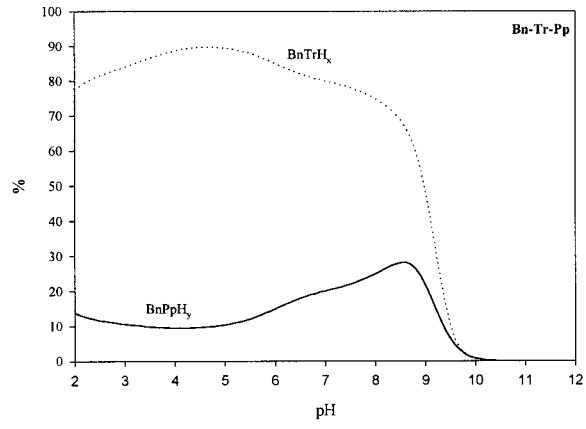
Bn-Tr-Pp
BnTrHx
BnPpHy
%
pH

a'

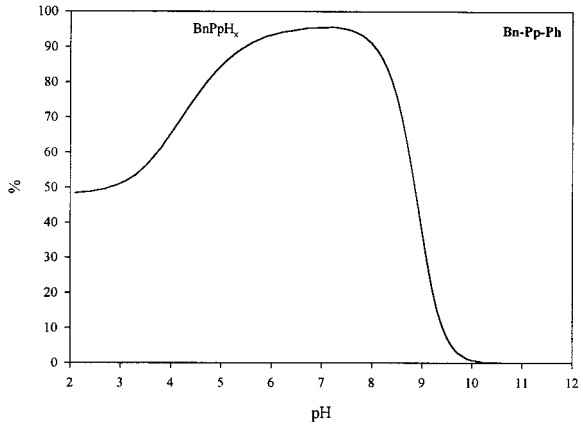
Bn-Pp-Ph
BnPpHx
%
pH

b'

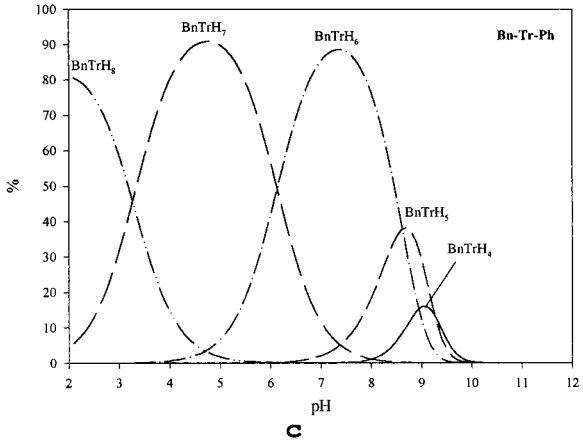
Bn-Tr-Ph
BnTrH8
BnTrH7
BnTrH6
BnTrH5
BnTrH4
%
pH

c

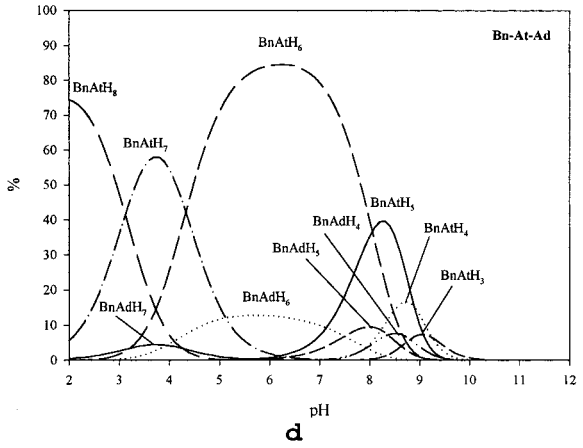
Bn-At-Ad
BnAtH8
BnAtH6
BnAtH7
BnAtH5
BnAdH4
BnAtH4
BnAdH5
BnAtH3
BnAdH6
BnAdH7
%
pH

d

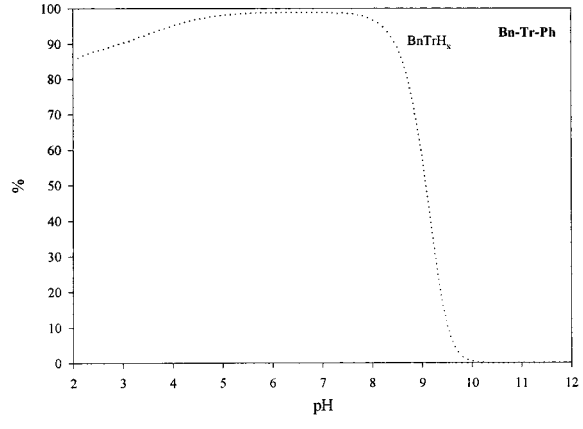
Bn-Tr-Ph
BnTrHx
%
pH

c'

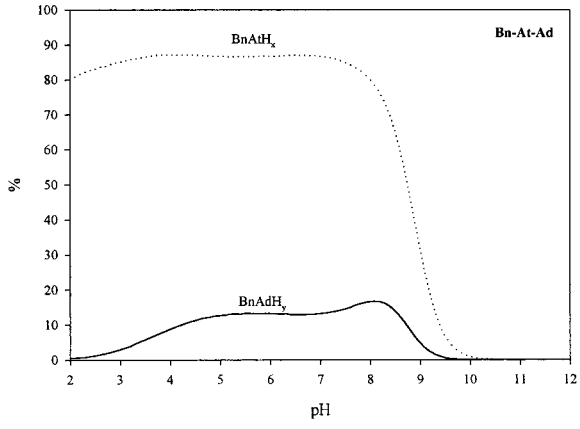
Bn-At-Ad
BnAtHx
BnAdHy
%
pH

d'

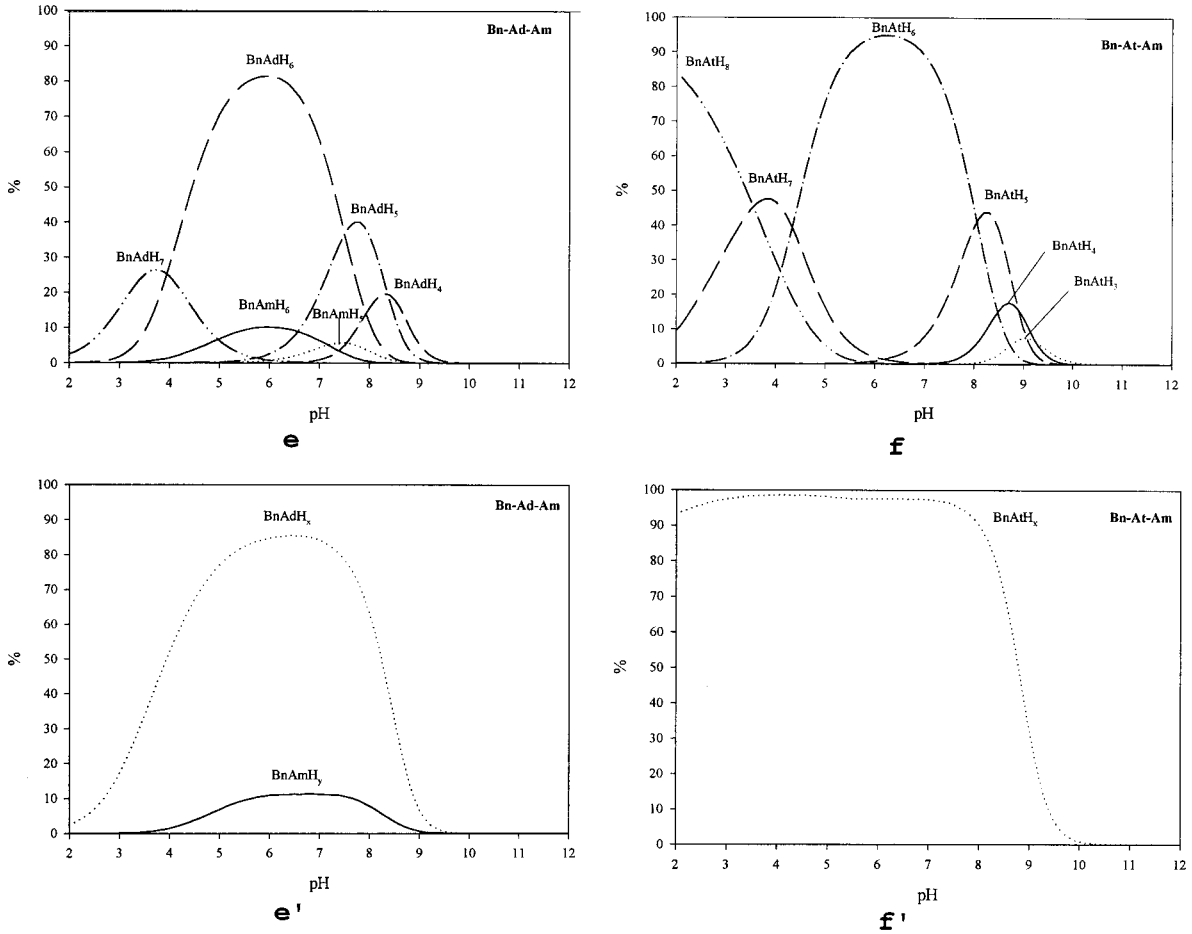

Figure 5. Competitive calculated species distribution diagrams for systems with equimolecular amounts of the Bn ligand and two phosphate (a−c) or two nucleotide (d−f) substrates together with their corresponding total species distribution diagrams (a′−f′).

The highest equilibrium constant for the present ternary recognition complexes H:Bn:Tr corresponds to the formation of the species H_6BnTr^+, log $K^R_6 = 8.60$. This complex can be formally described as a H_6Bn^{6+} positive cation bonded to a Tr^{5-} anion by Coulombic forces and hydrogen bonds. In this complex the Coulombic interactions and hydrogen bonding reach a maximum.

There is a gradual decrease of log K^R_i from $i = 6$ to $i = 8$ where the Coulombic interactions decrease as well as the potential hydrogen-bonding contributions. From $i = 6$ to $i = 4$ log K^R_i decreases corresponding to a decrease of both potential H-bonding and formal Coulombic interactions between host and guest.

The interaction of the Bn ligand with the other substrates namely diphosphate, monophosphate, and the nucleotides At, Ad, and Am has also been studied and the formation constants for the species obtained in each case are reported in Table 5.

The values obtained in the mathematical treatment confirm the qualitative assessment made above with regard to the direct relationship between the divergence of the real potentiometric curves with respect to the curves calculated with no interaction (Figure 3A). Thus when the formation constants for species with general formula H_6BnS^{n+} are compared (S = Tr, Pp, Ph, At, Ad, Am), it is found that the log *K*'s decreases in the manner Tr (8.60) > Pp (7.85) > Ph (3.50) for the phosphates and At (7.13) > Ad (5.37) > Am (3.62) for the nucleotides. This trend is maintained over the ternary species with substrates having the same degree of protonation H_iBnS. This can be graphically observed in Figure 4A where log K^R_i values are plotted versus *n*H, the species with various degrees of protonation. In the graph it is also clearly seen that the ternary species containing six protons, H_6BnS^{n+}, always have the higher recognition constant irrespective of the substrate type either phosphate or nucleotide. The latter suggests that in the present case Coulombic interactions play a predominant role in the molecular recognition phenomenon.

The fully deprotonated phosphate substrate (PO_4^{3-}) is a very strong base having a log *K* value for its first protonation of 11.63 (Table 3). The species distribution diagram for the monophosphate system alone indicates that the formation of the PO_4^{3-} species starts being significant above p[H] 10.5.[9] For the other 5 substrates described in the present work, in all cases the respective fully deprotonated species are already significant at p[H] 7.5. As stated above, at high p[H] the experimental potentiometric curves merge with the calculated (vide supra) assuming there is no interaction between ligand and substrate. As a consequence of this, in the species distribution diagram for all systems it is found that above p[H] 9 the predominant species are the free ligands and substrates. Given the specific nature of the monophosphate substrate and the experimental working conditions, only its second and third protonation constants will be relevant for the description of ternary complexes. Thus the Ph abbreviation in the ternary complexes described in the present work is used to symbolize the HPO_4^{2-} species.

When log *K* values for complexes of the type H_6BnS^{n+} (S = Tr, Pp, Ph and At, Ad, Am), bearing the same number of relevant acidic protons, are compared, it is found that for At,

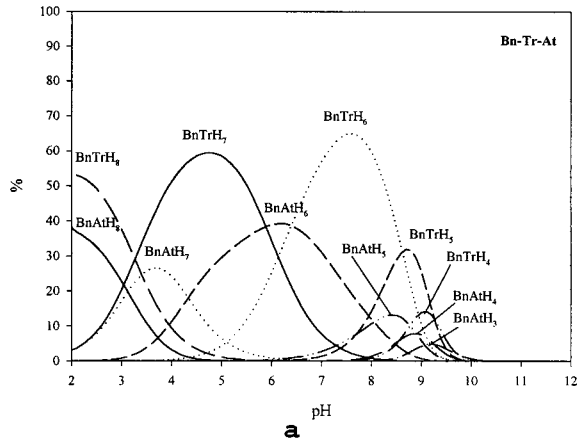
Bn-Tr-At
BnTrH8
BnTrH7
BnTrH6
BnAtH8
BnAtH7
BnAtH6
BnAtH5
BnTrH5
BnTrH4
BnAtH4
BnAtH3
%
pH

a

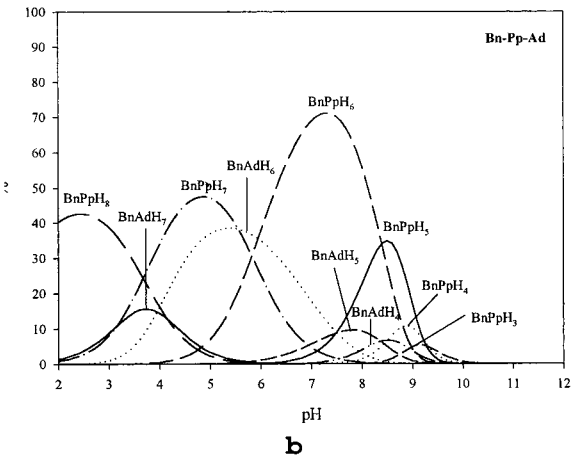
Bn-Pp-Ad
BnPpH6
BnAdH6
BnPpH8
BnPpH7
BnAdH7
BnPpH5
BnAdH5
BnPpH4
BnAdH4
BnPpH3
%
pH

b

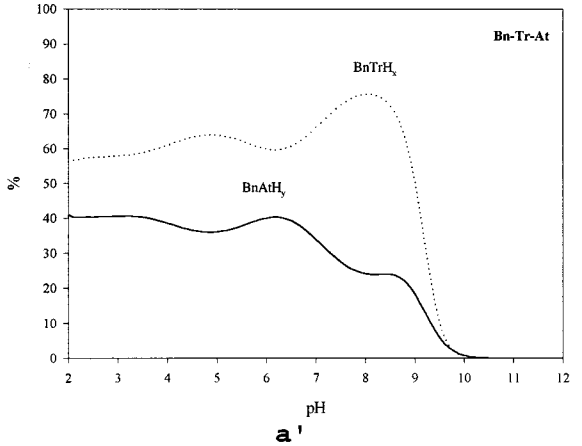
Bn-Tr-At
BnTrHx
BnAtHy
%
pH

a'

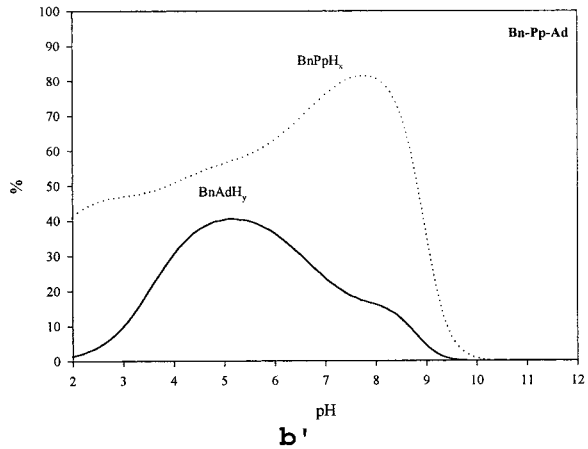
Bn-Pp-Ad
BnPpHx
BnAdHy
%
pH

b'

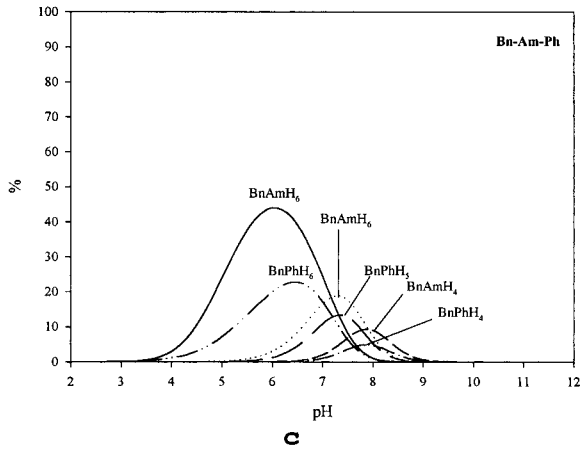
Bn-Am-Ph
BnAmH6
BnAmH6
BnPhH6
BnPhH5
BnAmH4
BnPhH4
%
pH

c

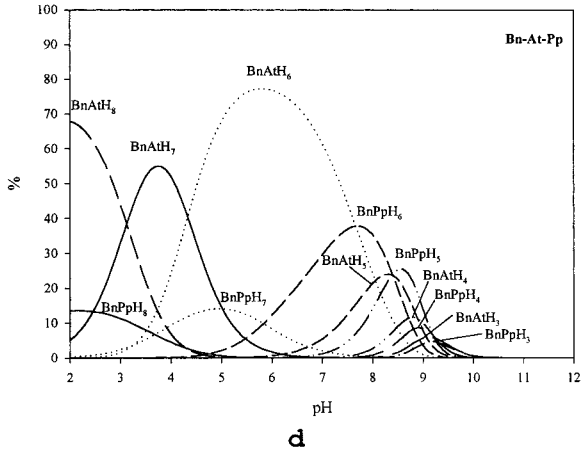
Bn-At-Pp
BnAtH6
BnAtH8
BnAtH7
BnPpH6
BnAtH5
BnPpH5
BnAtH4
BnPpH7
BnPpH8
BnPpH4
BnAtH3
BnPpH3
%
pH

d

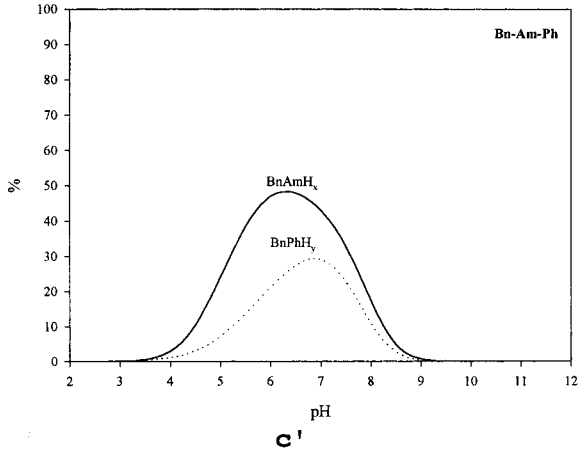
Bn-Am-Ph
BnAmHx
BnPhHy
%
pH

c'

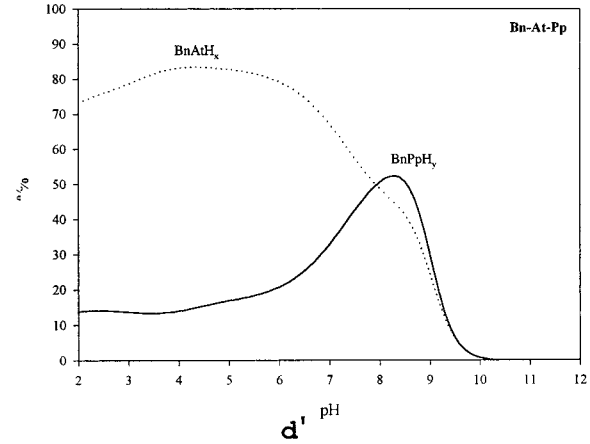
Bn-At-Pp
BnAtHx
BnPpHy
%
pH

d'

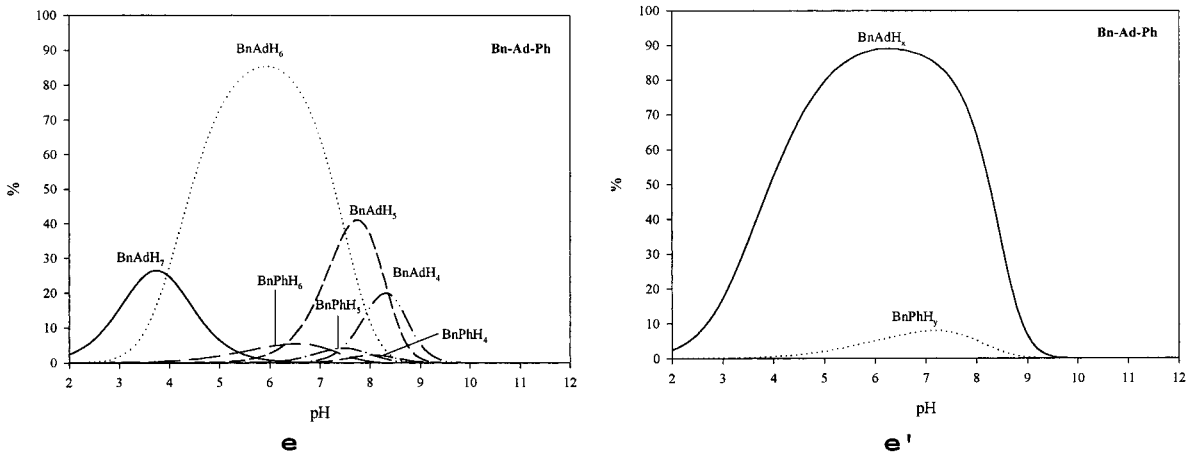

Figure 6. Competitive calculated species distribution diagrams for systems with equimolecular amounts of the Bn ligand, one phosphate, and one nucleotide (a−e) substrates together with their corresponding total species distribution diagrams (a′−e′).

Ad, and Am there is a regular decrease of approximately 1.75 log units for the formation constants that can be assigned mainly to the progressive decrease 4−, 3−, and 2−, respectively, of their Coulombic charge. For the phosphates from Tr to Pp the Coulombic charge decreases 1 unit, but from Pp to Ph it decreases 2 units; this fact is strongly manifested in their logs of protonation constants that decrease first 0.75 log units and then 4.35 log units, respectively (see Table 5 and Figure 4).

When nucleotides and inorganic phosphates are compared, log *K* values are closer for those systems that have the same Coulombic interactions than for substrates that have the same number of phosphate units. Thus log *K* values for the H_6BnS^{n+} systems are closer between At (7.13) and Pp (7.85) than between At (7.13) and Tr (8.60), thus manifesting the predominance of the ionic bonding over the different types of interactions that contribute to the overall bonding. This is further corroborated with the relatively similar log *K* values for Ph (HPO_4^{2-}) (3.50) and Am (3.62) for similar species.

Figure 3B shows the species distribution diagram as a function of p[H] obtained for the 1:1 Bn−S systems. As stated above for the Bn−Tr system ternary species predominate over the p[H] range 2−9. The decrease of the log *K* values observed for the Pp and Ph substrates in the Bn−Pp and Bn−Ph systems is clearly manifested in those diagrams. For Bn−Pp, the zone of predominance of the ternary complexes is now lower, from p[H] 4 to p[H] 9, whereas for the Bn−Ph system predomination is dramatically reduced to a mere half a p[H] unit from 6.2 to 6.7. A similar trend is found for the distribution species diagrams of the Bn−nucleotide systems: for the system Bn−At the zone of predominance of the ternary species is from p[H] 2 to 8.5 while for Bn−Ad is from 4 to 8 and for the Bn−Am system is from 5.5 to 6.9.

Bn Competitive Diagrams and Selectivity. Figure 5a−f presents calculated species distribution diagrams for systems with equimolecular amounts of the Bn ligand and two substrates together with their corresponding total species (defined as the summation of species containing a particular nucleotide or phosphate) distribution diagrams to show competition for various guests (Figure 5a′−f′). For the Bn−Tr−Pp competitive system, H:Bn:Tr species predominate over H:Bn:Pp species, within the p[H] range 2−9 as a consequence of the higher binding constants found for the Bn−Tr system compared to the Bn−Pp system. At p[H] higher than 9, the predominant species is the free ligand Bn which is not plotted in the graph. Similar diagrams can be obtained for combinations of equimolecular amounts of any two substrates with Bn as depicted in Figure 5. The total species distribution diagram gives a graphical view of the selectivity of the Bn ligand for two different substrates as a function of p[H]. For instance for the Bn−Tr−Pp competitive system (Figure 5a′) at p[H] 2 more than 92% of the Bn ligand would be complexed with the two substrates, 78% forming H:Bn:Tr species and 14% forming H:Bn:Pp species. That implies a selectivity of over 84.8% in favor of the Tr complexation against Pp. The selectivity of the Bn ligand for Tr over Pp reaches a maximum at p[H] 4.8 with a value of 90.2%. On the other hand, at p[H] 8.5 the selectivity of Bn for those two substrates reaches a minimum with a value of 70.8%.

Figure 5b,b′ displays the species distribution and total distribution species diagrams, respectively, calculated for the Bn−Pp−Ph system. In this case the H:Bn:Pp type of species strongly predominate over the H:Bn:Ph as expected since the recognition constants for the latter are 2−4 log units lower than for the former. From p[H] 2 to 4 H:Bn:Ph species are practically absent, and therefore, the only species present contain the Pp substrate. From p[H] 4 to 8 H_i:Bn:Ph species are observable reaching a maximum at p[H] 6.8 with a selectivity of 95.9%. A more dramatic effect is observed for the Bn−Tr−Ph system (Figure 5c,c′) where the selectivity value obtained is 99.9% in the p[H] range 6−7.5.

Figure 5 also contains the corresponding diagrams for the Bn−S−S′ systems with nucleotides. Relatively similar trends are observed when carrying out a comparative analysis like the one performed with the inorganic phosphates, perhaps the most remarkable difference being the absence of complex species at lower p[H] (p[H] 2) for the system Bn−Ad−Am in contrast with Bn−Pp−Ph where nearly 50% of the ligand would be bonded to the substrate. It is also interesting to point out the similarity among their calculated species distribution diagrams (Figure 5d−f), which is due to the fact that the relevant protonation constants K^H_1 and K^H_2 of the three nucleotides differ by less than 0.3 and 0.1 log units, respectively.

Figure 6 contains a cross examination of comparative diagrams for Bn−S−S′ systems with S being a phosphate type of substrate and S′ being a nucleotide. For substrates containing the same number of phosphorus atoms the phosphates always have higher abundance than the nucleotides given their higher binding constants except for the Bn−Ph−Am system reflecting the singularity of the monophosphate substrate. Figure 6d,d′ contains graphs for the system Bn−Pp−At, that is, substrates with the same formal Coulombic charge but with two and three phosphorus atoms, respectively. In the graph it can be observed

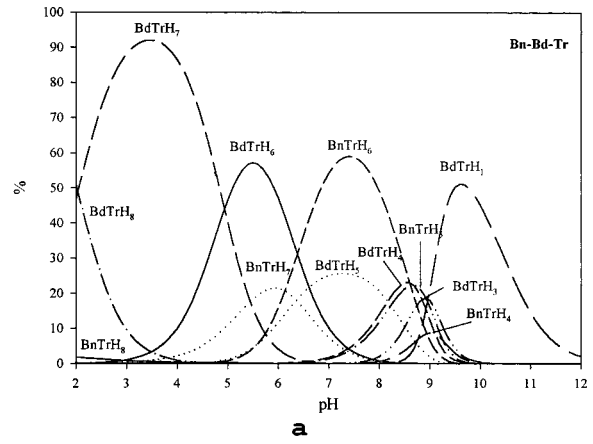
Bn-Bd-Tr
BdTrH7
BdTrH6
BnTrH6
BdTrH1
BdTrH8
BnTrH7
BdTrH5
BdTrH2
BnTrH5
BdTrH3
BnTrH4
BnTrH8
%
pH

a

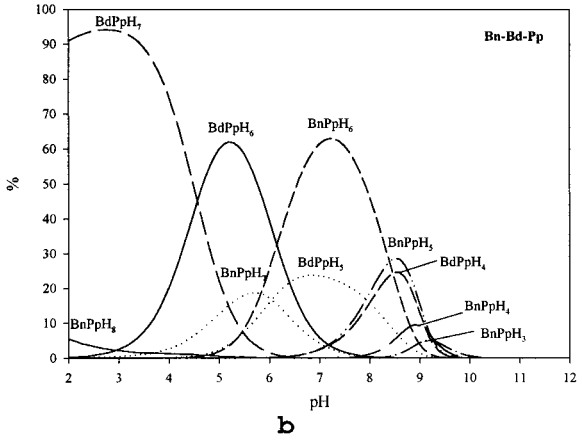
Bn-Bd-Pp
BdPpH7
BdPpH6
BnPpH6
BnPpH5
BnPpH7
BdPpH5
BdPpH4
BnPpH4
BnPpH8
BnPpH3
%
pH

b

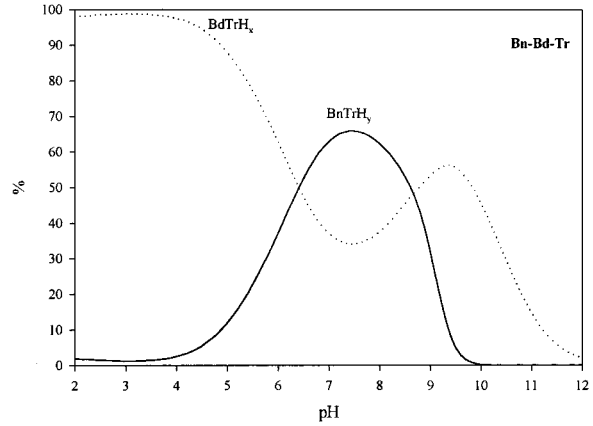
Bn-Bd-Tr
BdTrHx
BnTrHy
%
pH

a'

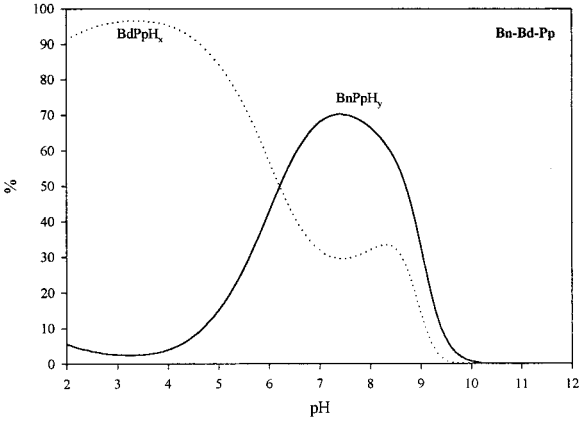
Bn-Bd-Pp
BdPpHx
BnPpHy
%
pH

b'

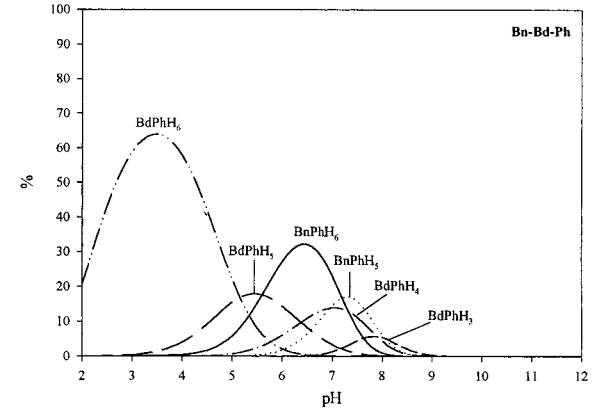
Bn-Bd-Ph
BdPhH6
BnPhH6
BdPhH5
BnPhH5
BdPhH4
BdPhH3
%
pH

c

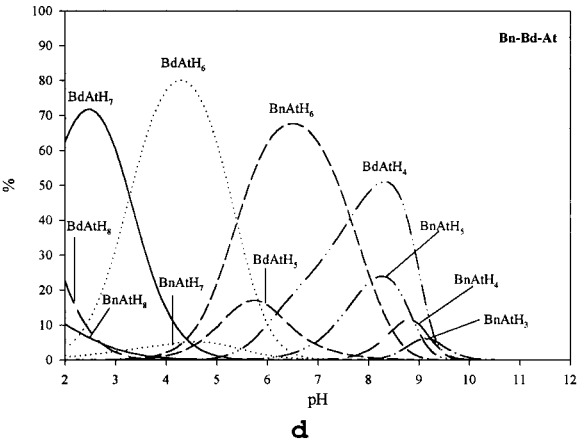
Bn-Bd-At
BdAtH6
BdAtH7
BnAtH6
BdAtH4
BdAtH8
BnAtH5
BdAtH5
BnAtH7
BnAtH4
BnAtH8
BnAtH3
%
pH

d

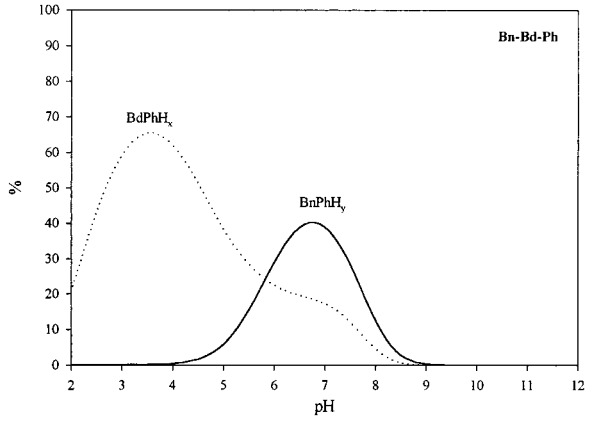
Bn-Bd-Ph
BdPhHx
BnPhHy
%
pH

c'

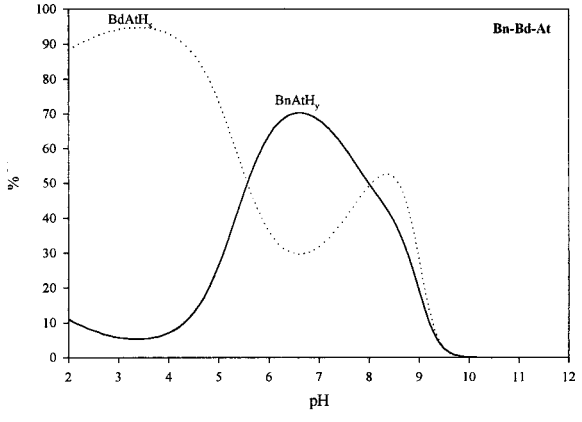
Bn-Bd-At
BdAtHx
BnAtHy
%
pH

d'

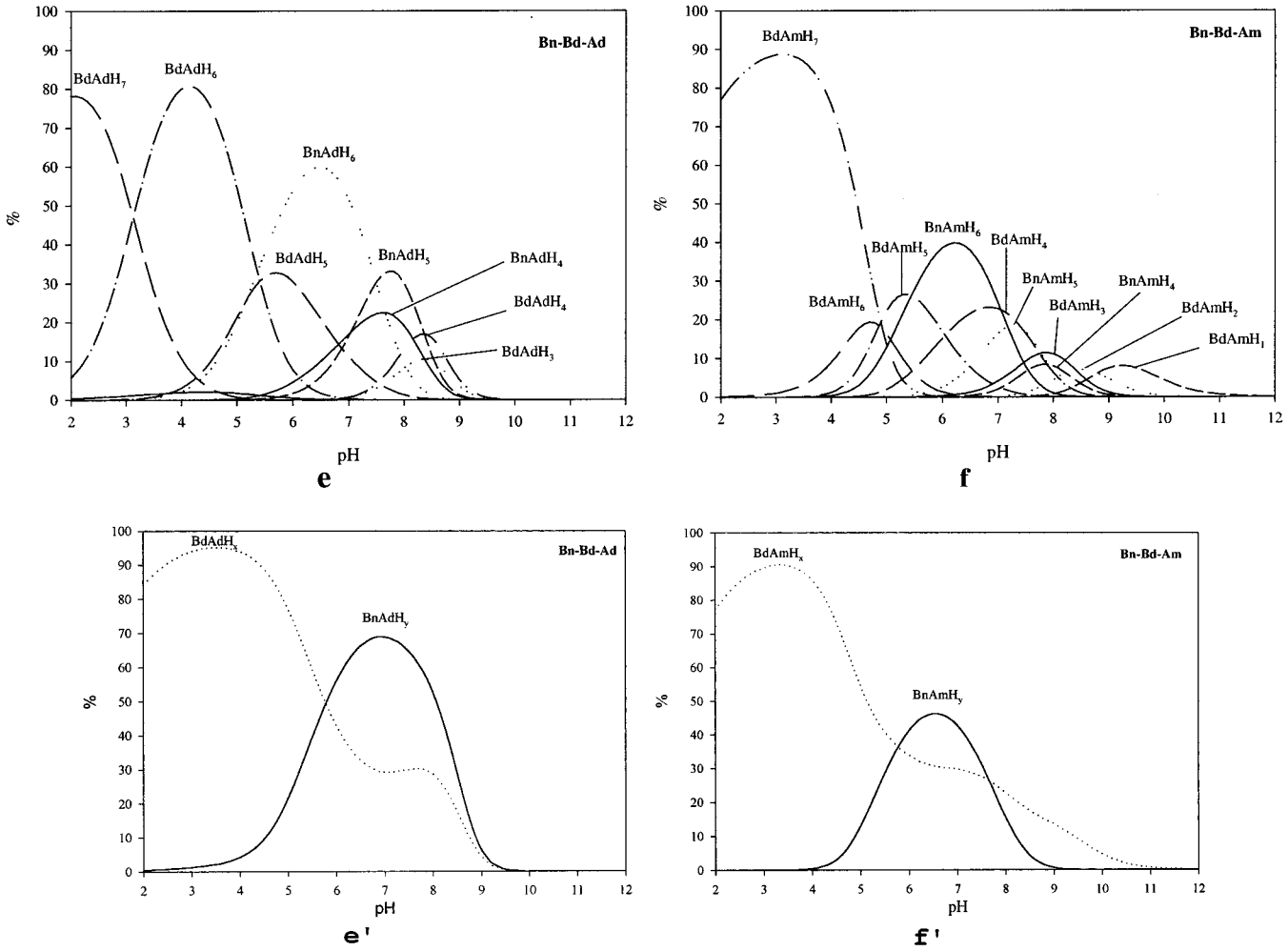

Figure 7. Competitive calculated species distribution diagrams for systems with equimolecular amounts of the Bn ligand, the Bd ligand, and one phosphate or nucleotide substrate (Bn−Bd−S) (a−f) together with their corresponding total species distribution diagrams (a′−f′).

that in the 7.5−8.5 p[H] range the nucleotide has higher affinity for the ligand than the diphosphate.

Bn vs Bd Competitive Systems. To have a complete description of the factors influencing the molecular recognition phenomena between the macrocycles and the substrates it is important to compare the results of the present work with the results obtained for a similar macrocycle containing a smaller cavity such as the Bd ligand. Assuming that Bd could have an extended conformation similar to the one presented in the crystal structure of Bn (see Figure 1), that is with all aliphatic C and N atoms lying roughly in the same plane, the removal of 4 C atoms of this cavity will provoke a shrinking of about 20% of the cavity size. On the other hand, the overall basicity of the Bd ligand is 10 orders of magnitude lower than that of the Bn ligand, as reported in Table 3. As a consequence of those two factors, the formation of tertiary species with Bd is always from 2 to 5 orders of magnitude higher (see Table 5 and Figure 4). However, when the calculated species distribution diagrams and the total species distribution diagrams for Bn−Bd−S competitive systems are compared (see Figure 7), the zone of predominance of the two ligands depends on the p[H]. For phosphates the H:Bd:S species would predominate over the p[H] 2−6 range whereas H:Bn:S species would predominate from p[H] 6 to 9. For the nucleotides H:Bd:S species would predominate over the p[H] 2−5.5 and 7.8−9 ranges whereas H:Bn:S species would predominate from p[H] 5.5 to 7.8. The predominance of H:Bn:S species over H:Bd:S species is due to the different distribution species of the free ligand as a function of p[H], as can be observed in Figure 2. From p[H] 2 to 5.5 only the hexaprotonated species H_6Bn^{6+} competes with the corresponding hexa-, penta-, and tetraprotonated species of Bd. Thus in this p[H] zone H:Bd:S species are always favored with regard to H:Bn:S species. From p[H] 5.5 to 8 in the Bn case the penta-, tetra-, and triprotonated species are predominant while within the same p[H] range only the tetra and triprotonated species are expressed thus favoring the formation of H:Bn:S type of species over H:Bd:S even though the latter have higher formation constants.

Finally it worth mentioning that, for the Bd−S systems, the different number of protonated species found in the solution equilibria is generally higher than for the Bn−S system. This especially holds true for the Am nucleotide where three different protonated complex species are detected with Bn whereas seven are found for Bd under similar conditions. This is no doubt due to the higher formation constants displayed for the latter with regard to the former.

Summary and Conclusions. Molecular recognition phenomena between the hexaazamacrocyclic ligands Bn and Bd and nucleotide and phosphate type of substrates are strongly dependent on the size and nature of the macrocyclic ligand (L) and the substrate (S). Bonding between the ligand and substrate can be rationalized in terms of hydrogen bonding and Coulombic interactions with the latter playing a predominant role. As a consequence, the strength of the ternary complexes H:L:S follows the order Tr > Pp > Ph and At > Ad > Am. Furthermore when inorganic phosphates and nucleotides are compared, the strength of the H:Bn:Pp and H:Bn:At complexes

(substrates with similar Coulombic charge) are closer than for H:Bn:Tr and H:Bn:At (substrates with the same number of phosphorus atoms). In comparative conditions Bd always forms complexes with higher formation constants than Bn. However, the predominance of Bn or Bd ternary species is strongly dependent on p[H]. Finally, the conclusions drawn here agree well with those obtained previously for related macrocyclic receptors and phosphates.[4,5]

Acknowledgment. This research has been supported by the Robert A. Welch Foundation under Grant No. A259 and by the DGICYT of Spain through Projects PB96-0467 and QUI96-C103-03. The CIRIT of Catalunya is also gratefully acknowledged for an aid SGR-3102-UG-01. C.A. thanks the University of Girona for the allocation of a doctoral grant.

IC990818P